

# Rates and Rhythms: A Synergistic View of Frequency and Temporal Coding in Neuronal Networks

Matt Ainsworth,<sup>1</sup> Shane Lee,<sup>3,4</sup> Mark O. Cunningham,<sup>1</sup> Roger D. Traub,<sup>2</sup> Nancy J. Kopell,<sup>3</sup> and Miles A. Whittington<sup>1,\*</sup>

<sup>1</sup>Institute of Neuroscience, Newcastle University, Newcastle upon Tyne, NE2 4HH, UK

<sup>2</sup>Department of Physical Sciences, IBM T.J. Watson Research Center, Yorktown Heights, NY 10598, USA

<sup>3</sup>Department of Mathematics and Statistics, Boston University, Boston, MA 02215, USA

<sup>4</sup>Present address: Department of Neuroscience, Brown University, Providence RI 02912, USA

\*Correspondence: [m.a.whittington@ncl.ac.uk](mailto:m.a.whittington@ncl.ac.uk)

<http://dx.doi.org/10.1016/j.neuron.2012.08.004>

In the CNS, activity of individual neurons has a small but quantifiable relationship to sensory representations and motor outputs. Coactivation of a few 10s to 100s of neurons can code sensory inputs and behavioral task performance within psychophysical limits. However, in a sea of sensory inputs and demand for complex motor outputs how is the activity of such small subpopulations of neurons organized? Two theories dominate in this respect: increases in spike rate (rate coding) and sharpening of the coincidence of spiking in active neurons (temporal coding). Both have computational advantages and are far from mutually exclusive. Here, we review evidence for a bias in neuronal circuits toward temporal coding and the coexistence of rate and temporal coding during population rhythm generation. The coincident expression of multiple types of gamma rhythm in sensory cortex suggests a mechanistic substrate for combining rate and temporal codes on the basis of stimulus strength.

In determining how the brain codes for sensory inputs and motor outputs two types of measurement dominate the literature: the outputs (action potentials or units) of identified neurons or groups thereof and the local mean synaptic inputs (local-, far- or extracranial field potentials). Patterns observed in either measurement are clearly related; being dependent on the computational processes occurring in compartments of individual neurons and distributed networks. However, which, if any, of the patterns of activity observed in either type of measurement correspond to psychophysical performance in an organism remains open to a great deal of debate. This review attempts to put forward a synergistic view whereby the interrelationship between rates of neuronal output are considered with respect to the frequencies and types of synaptic input in neocortex. We first consider whether the behavior of individual neocortical neurons may relate to cognitive and/or motor performance, arguing that the interconnectedness of neurons strongly favors population coding. Working from this argument we then consider how many neuron's outputs may constitute such a population code, what brings the population together, what features of the population's inputs and outputs are most psychophysically salient, and finally how this relates to patterns of short and long term plasticity in cortex.

## Is a Neuronal Network a Valid Functional Entity?

Individual neurons make a quantifiable contribution to the function of simple nervous systems (e.g., McAllister et al., 1983). But when a nervous system consists of not ca.  $10^2$  neurons but  $10^{11}$  neurons, as in man, do individual neurons still matter? It is well recognized that single neuron spiking contributes to the code for specific orientations of features in specific regions

of the visual field (Hubel and Wiesel, 1959). Similarly, discrete spectrotemporal properties of auditory sensory presentations can be seen to be represented by the spiking of individual cortical neurons (Fritz et al., 2003; Figure 1). Single neurons may also be seen to code for higher-order sensory object properties on occasion (e.g., Logothetis et al., 1995; Quiroga et al., 2005), and spike outputs from single neurons may influence the motor act of whisking in rodents (Brecht et al., 2004; Figure 1).

However, individual neurons in the cortex are densely interconnected, both locally and distally, with a disparate population of other neuronal subtypes. In addition, single-modality sensory objects have many features that need to be coded together, and motor outputs are often extremely complex. It is also rare for just one neuron to be activated by a single stimulus or stimulus property (see Braitenberg, 1978; Abeles, 1988; Duret et al., 2006) but far more common that neurons may respond to multiple events in a sensory task (Vaadia et al., 1995). In addition, many sensory inputs present multimodally and thus require the activation of numerous, spatially separate cortical regions (Singer, 2010). Thus, despite demonstrations of a clear role for individual neurons, the evidence for multiple neuronal involvement in sensory processing and motor activity has led to the suggestion that population coding is "inevitable" (Sakurai, 1998).

## The Size and Nature of a Population Code

If the output of a single neuron alone is rarely, if ever, sufficient to generate a useful representation of sensory input or motor output, then how many neurons are needed? In studies focusing on synaptic inputs to cerebellar granule cells during vestibular stimulation a highly precise relationship between individual

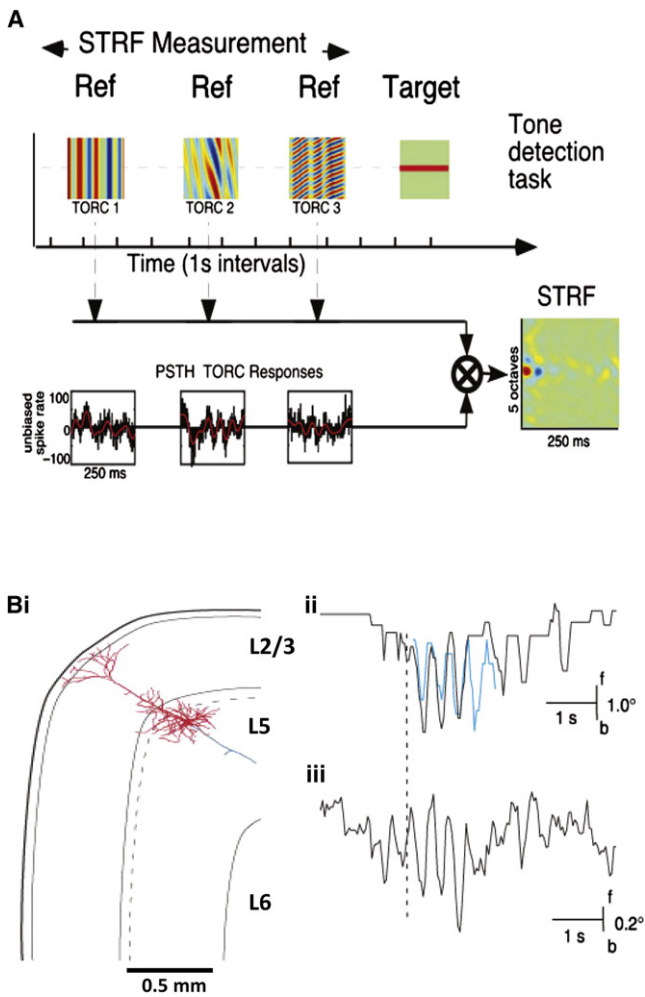


**Figure 1. Contribution of Single Neurons to Sensory Input Coding and Motor Output Generation**  
 (A) Individual primary auditory cortex neurons respond to complex sounds varying in time and frequency. Specific components of presented auditory stimuli are reflected in the spectrotemporal response field (STRF) of each neuron. The STRF shown was estimated by cross-correlation of the spectrogram of the reference stimuli delivered (temporally orthogonal ripple combinations (TORCs) with the post-stimulus time histogram of the neurons unit activity (PSTH). In this study the authors used behavioral reward to show that neuronal STRFs could be tuned to pure tone target stimuli (adapted from Fritz et al., 2003).  
 (B) Single layer 5 neuron outputs in motor cortex can induce whisker movement in rat. (i) The neuron shown was stimulated to generate 10 action potentials at 50 Hz and induced the phasic pattern of movement only in whisker D1 shown in (ii). Note the two trials illustrated (black and blue lines) produced movements in phase. (iii) Average of 15 trials showing the well conserved motor pattern induced by the single cell. Figure reproduced from Brecht et al. (2004).

neuron input and the vector of associated movement was seen (Arenz et al., 2008). These authors estimated that as few as 100 synapses were needed to provide a resolution of sensory input approaching psychophysical limits (Figure 2). The authors' own caveat to this work is that the cerebellar granule cell used in this study is a simple neuron with only a few, well-defined inputs. More complex cortical neurons with large dendritic arbors

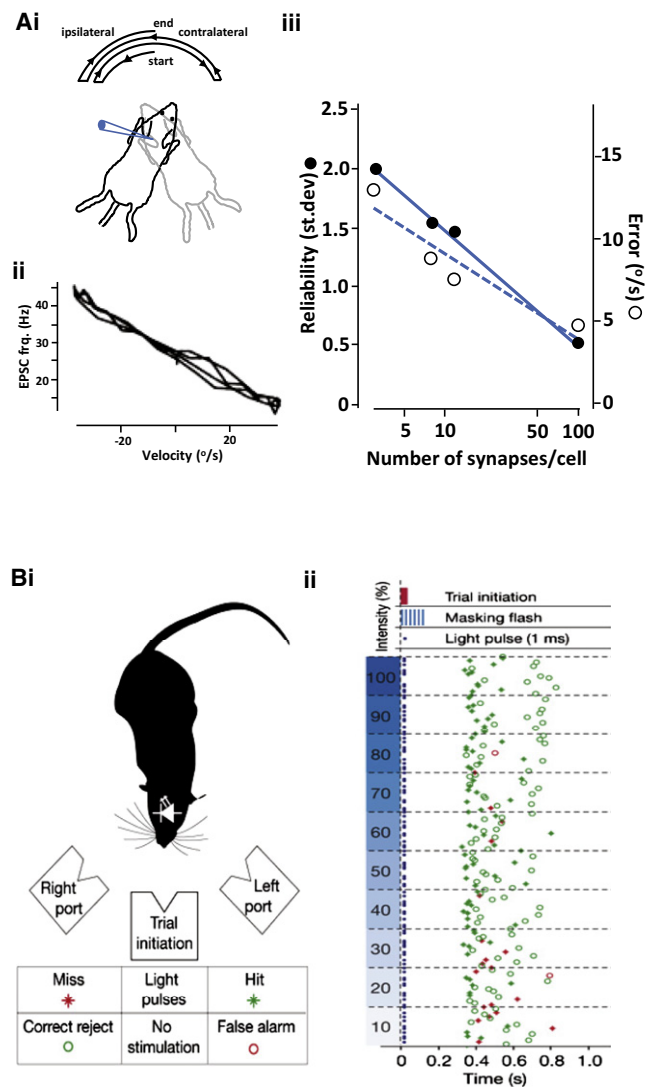


**Figure 2. Small Populations of Active Neurons Are Sufficient to Accurately Represent Sensory Input**  
 (A) ca.100 neurons can convey velocity information about horizontal head movement at the mossy fiber-granule cell (MF-GC) synapse in cerebellum. (i) The horizontal stimulus used to drive vestibular inputs. (ii) EPSC frequency in a single granule cell correlates linearly with velocity and direction of movement. (iii) Bayesian reconstruction algorithm results estimating the accuracy of motion representation by MF-GC EPSCs. Note the reliability (i.e., decreased standard deviation of the movement error) and accuracy (decreased mean error) increased dramatically to within psychophysical limits ( $4^{\circ}$ – $8^{\circ}$ /s) as the number of synapses considered increased from just a few to ca. 100. (Adapted from Arenz et al., 2008).  
 (B) Stimulation of a few 100 channelrhodopsin expressing neurons in somatosensory cortex can accurately induce a learned behavior (reward seeking). (i) In Huber et al. (2008) mice initiated a behavioral trial by activating the central port. If cortical neurons were activated by photostimulation the mouse was rewarded if it chose the left port (hit, green star). If no stimulation was given the mouse was rewarded if it chose the right port (reject, green circle). (ii) Example session data for a single photostimulus present (blue dot) or absent. Each block of responses shows 20 trials at the light intensity shown on the left. Reproduced from Huber et al. (2008).

may require the integration of far more inputs. However, using precisely targeted photostimulation of such complex neurons in superficial somatosensory cortex in mice a similar magnitude

of neuronal involvement correlated with a measure of psychophysical salience (Huber et al., 2008; Figure 2). Following training, a correct behavioral response could be detected in mice with single action potentials being generated in as few as 300 neurons. This size of active population fell even further if individual neurons were stimulated to generate short trains of multiple action potentials (see below).

From an anatomical perspective, assuming interconnectivity is required between cofunctioning neurons, evidence points to neuronal populations being highly distributed entities. Despite the tens of thousands of synapses on individual cortical principal cells, very few come from local excitatory neurons. Estimates for connectivity rates in pairs of principal cells within cortical regions range from ca. 1:25 to 1:400 (Deuchars and Thomson, 1996; Andersen, 1995). Thus, for every 1,000 neurons, each one is likely to receive connections from approximately 2–40 of its neighbors. Low specific connectivity rates also appear when considering longer range interactions. In primary sensory areas, only ca. 5% of synapses arise from ascending inputs (Peters and Payne, 1993), with similar proportions for inputs from other distal cortical regions (Anderson et al., 1998; Budd, 1998). Estimates of interconnectivity suggest a “chorus” of ca. 20–30 different anatomical origins for inputs to a single cortical region (Scannell and Young, 1999; Young, 2000). Efficacy of single excitatory synapses onto principal cells is also weak in most cases. Measures range from ca. 1 mV down to 0.1 mV (Holmgren et al., 2003; Williams and Atkinson, 2007) at rest in most principal cells, and become even less in the presence of neuromodulators associated with the wake, attentive state (e.g., Levy et al., 2006).

These properties of neuronal connectivity allow us to suggest a lower bound on the size of cell assemblies. Assuming linear heterosynaptic summation of inputs coincident within a few milliseconds (but see below), a single downstream target neuron could be made generate an output from a synchronous, upstream assembly consisting of a few 10 s to 100 s of member neurons depending on membrane potential and conductance state—a figure that fits well with the functional studies described above. Therefore, for a general estimate of assembly size these data suggest a spatially distributed population of order no less than  $10^1$ – $10^2$  neurons, as also suggested for local assembly formation during gamma rhythms (Börgers et al., 2012). However, principal neurons may also influence each other indirectly via activation of inhibitory interneurons and gap junction-mediated electrical synapses (Hormuzdi et al., 2001)—both predominantly local phenomena. Neighboring neurons appear to share many of their coding properties (Smith and Häusser, 2010), and local inhibition and gap junctional communication are both capable of organizing spike outputs in time (Pouille and Scanziani, 2001; Traub et al., 2003). Thus many different “copies” of distributed, excitatory functional populations may concurrently arise from activation of a single primary sensory area *without* the existence of any direct Hebbian excitatory connectivity between their member neurons.

### What Brings a Population Together?

The predominant feature of population coding is that member neurons must act together in time. This is considered for the

most part to mean neurons generate outputs synchronously (Eckhorn et al., 1988; Gray and Singer, 1989; Deppisch et al., 1994). Thus, a coactive neuronal population—an assembly of neurons—exists in both time (the relative temporal relationship between outputs from member neurons) and space (the physical location of the member neurons). First we consider these features separately.

In response to sensory input the incidence of near-synchronous spike generation among multiple neurons is very common and may even be the defining feature of the cortical representation of information received (Engel et al., 2001; Freiwald et al., 2001). This is, at first glance, surprising, since individual spike times in cortical neurons are highly variable (Softky and Koch, 1993; Shadlen and Newsome, 1994, 1995), a property proposed to be related to the relative distributions, in time, of near-random patterns of many thousands of inhibitory and excitatory inputs. In this scheme, each neuron effectively generates an output in the rare instances when excitation is not balanced by inhibition, a phenomenon analogous to statistical coincidence detection at a single-neuron level (Softky, 1995). Within such a scheme the probability of many multiple neurons generating outputs synchronously is extremely low. Nevertheless, such coincidences in spike generation are seen to some extent even in cortex in the absence of salient stimulus presentation (Arieli et al., 1995). It should also be noted that the fact that oscillations are observable at all with macroscopic electrodes in extracranial recordings indicates a high degree of synchrony over at least several centimeters in neocortex is commonplace. Thus, some mechanism is needed to produce this near-synchrony.

How precise does this synchrony have to be to be functionally meaningful? The processes underlying assembly formation in time appear highly non-stationary, with significant synchronization among populations of neurons often observed over only short epochs (e.g., Riehle et al., 2000), often iteratively on time-scales corresponding to the gamma-theta EEG period range (20–200 ms (Singer and Gray, 1995; Harris et al., 2003; Figure 3). Even within such epochs, the degree of synchronization (alignment of spike times in multiple neurons making up the assembly of neurons) can be time variable, so it is important to consider just how much “jitter” in relative timing of spikes can be tolerated and still be able to consider assembly member neurons to be “acting together.” If cortical neurons are fed inputs modeled upon the faster components of postsynaptic events, they can generate spikes with precision in the order of one millisecond or less (Mainen and Sejnowski, 1995). Ascending cortical inputs have been shown to be most efficient in generating cortical responses when presented on a timescale of ca. 5 ms for both visual (Wang, 2010) and auditory (Kayser et al., 2010) modalities. This order of temporal precision fits very well with synaptic biophysical properties relevant to intercommunication between cell assembly member neurons and their targets.

A further complication when considering what constitutes an assembly is that their identity, in terms of neurons involved and their spatial location, is often seen to evolve over time following stimulus (Beggs and Plenz, 2003). Avalanches of neuronal activity arise as a consequence of propagating local synchrony (Plenz and Thiagarajan, 2007). Taking all these factors into account, it is clear that an assembly (a functional neuronal

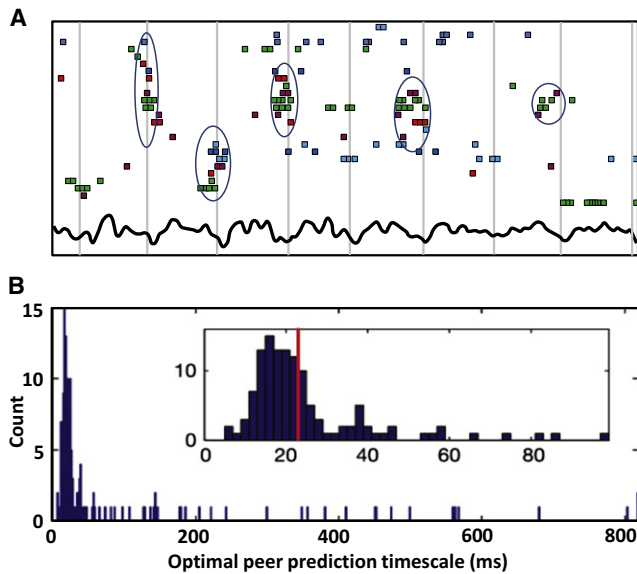


**Figure 3. Small Populations of Active Neurons (Assemblies) Are Temporally Organized**

(A) Raster plot of 25 extracellular spikes active over 1 s of field potential theta rhythm accompanying spatial exploration in hippocampus of the awake behaving rat. Vertical lines are referenced to the peak negativity of the theta field. Aligned with these periods of the on-going theta rhythm are repeatedly synchronous epochs of spike generation (circled). Color coding represents the spatial location of each raster (recording electrode number).

(B) Graph of enhancement of predictability of spike timing with peer activity over location alone versus relative time between spikes. The data show a very strong relationship between synchronous spike generation (assembly formation) and the period of the gamma rhythm (30–80 Hz). Figure adapted and reproduced with permission from Harris et al. (2003).

population) can be transient, highly spatiotemporally dynamic entities, very difficult to experimentally characterize but nevertheless of immense computational potential.

### Population Coding through Rate and Synchrony?

The original concept of a neuronal assembly comes from Hebb's seminal work (Hebb, 1949) in which he proposes cooperative activity within networks of interconnected neurons—essentially a population code for cortical function. Since then many variants have emerged, but most converge on a definition of the form: a set of neurons in a population that act together to perform a specific computational task (Palm, 1990; Eichenbaum, 1993).

There is much discussion over whether rate coding or temporal coding is used to represent sensory objects in populations of neurons in cortex. Experimental evidence for changes in firing rate only on change of perceptual state (e.g., Roelfsema et al., 2004; Lamme and Spekreijse, 1998) are as compelling as those which show changes in synchrony in the absence of firing rate changes (Fries et al., 1997; Engel et al., 2001; Womelsdorf et al., 2006). In most experiments, changes in both rate and spike correlations are observed concurrently (e.g., Biederlack et al., 2006), leading to the suggestion that rate changes in single neurons code for the discrete properties of a stimulus, whereas temporal code tags relatedness of each neuron's change in firing rate to form a broader percept (Singer, 2010). A number of reports suggest that as much as 90% of information in a stimulus

may be held in the rate code of active neurons (Aggelopoulos et al., 2005), while others suggest synchrony is key (deCharms and Merzenich, 1996).

Both rate and temporal codes are eminently capable of generating transient synchronous population events but do so in different ways. In superficial neocortex, gamma rhythms accompany sparse firing of individual principal cells (Cunningham et al., 2004). Somatic spike rates with modal zero values are common but assembly formation is still possible (Figure 6A). While sparse codes can generate assemblies by chance (see Shadlen and Movshon, 1999), the rate of coincident spike generation is far above this. The reason is simply that each principal cell, whether directly connected or not, shares a common pattern of phasic somatic inhibition (Whittington et al., 1995), limiting peak probability of spike generation to windows only a few milliseconds wide on every period of the underlying local population rhythm (Olufsen et al., 2003). Thus, while numbers of coactive neurons in a population are low, their temporal precision is very high (Figure 6C). In contrast, bursts of high spike rates in multiple neurons concurrently can also generate assemblies (Figure 6B), but in this case temporal precision is low and numbers of coactive neurons high (a function of mean population rate). Interspike intervals between peers approximate to a broad gamma function (Figure 6D) and one is left with the problems of quantifying just how precise the relative timing of spikes has to be to imply coding and deciding whether spikes lying outside this limit of precision are simply “wasted” or also subservice some coding function.

Between the above extremes of relationship between spike rate and synchrony, there is clearly a great deal of overlap between the rate and temporal coding schemes when considering temporal codes dictated by cortical rhythms. Synergy may also be evident. Near-synchronous generation of single action potentials in ca. 300 neurons in cortex produced behavioral responses equivalent to brief trains of 5 action potentials in only 60 neurons (Huber et al., 2008). In addition, population outputs organized by different frequencies of oscillation code for different visual feature scales in sensory objects (Smith et al., 2006) hand in hand with activation of rate changes in spatial frequency-selective neurons in visual cortex (De Valois et al., 1982). Action potential outputs at different frequencies (spike rates) imply time-varying phase relationships between coactive neurons (Markowitz et al., 2008) and seemingly uncorrelated spike pairs (over timescales associated with synchrony) can arise from robust rhythmic population activity at multiple, coexistent frequencies (Roopun et al., 2008). An interesting suggestion from a combination of spike rate and synchrony approaches has been proposed by Silberberg et al. (2004). Analysis of population activity when neurons are seen to output a range of different spike rates (distributed rate encoding) implicated “instantaneous population rate” as a coding strategy. In this case, it is the number of neurons generating spikes in a given time window that underlies a cortical code. With more and more brief time windows, this converges on a quantitative definition of transient neuronal assembly.

### Synaptic Limitations to Assembly Formation

To attempt to address whether assemblies generated by rate or temporal codes differ in their implications for cortical function

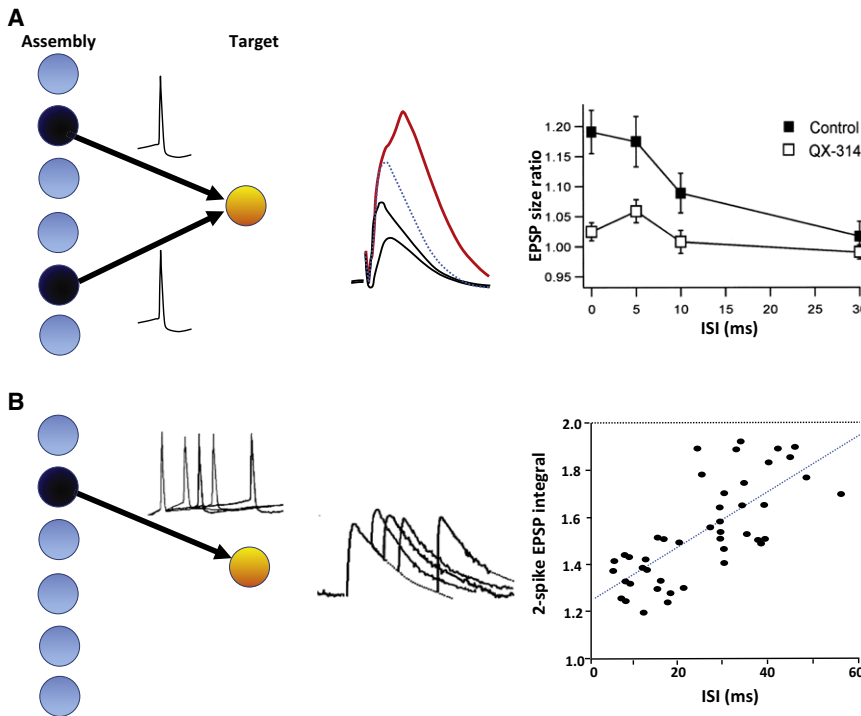


**Figure 4. Short-Term Excitatory Synaptic Plasticity Favors Downstream Effects of a Population Temporal Code over Single Neuronal Spike Rate Code**

(A) Supralinear summations of synchronous EPSPs. Cartoon illustrating a situation where two cortical neurons in assembly generate synchronous outputs converging on a single target neuron. Middle panel shows example data in which two EPSPs are received simultaneously from such synchronously active neuron pairs. The two individual EPSPs are shown as the black traces (with single presynaptic neuron activation). The algebraic sum of these two inputs to the target cell (assuming no interaction) is illustrated as the blue trace. Note, however, that the actual postsynaptic response from synchronous discharges in the presynaptic neurons is considerably larger than this predicted value (red trace). The right panel shows the dependence of supralinear summation on degree of presynaptic neuronal synchrony. The amplitude of the response to paired inputs is represented as the ratio between actual response observed and the predicted algebraic sum of the two individual responses (filled squares). Note the amplification of the postsynaptic response is maximal when spike generation is <5 ms time separated. This property of synchrony is dependent on postsynaptic intrinsic conductances, as shown by its near absence in QX314-loaded target neurons (open squares). Data reproduced, with permission, from Nettleton and Spain (2000).

(B) EPSPs generated by spike trains show frequency-dependent depression. In contrast to the amplification of near-synchronous EPSP from different neurons (A), driving a *single* presynaptic neuron to generate EPSP trains with interspike intervals corresponding to short heterosynaptic EPSP intervals results in synaptic depression. The left panel shows a cartoon of the situation being considered. The EPSP traces show 5 overlaid target neuron events when a single presynaptic neuron generates a single spike, or two spikes with intervals ranging from 10 ms to 40 ms. The right panel shows the pooled data from 22 paired recordings from layer 5 pyramidal cells in which the presynaptic neuron was stimulated to generate two spikes with intervals ranging from 5 to 55 ms. Note the overt, near-linear depression of the postsynaptic response to the second spike with decreasing ISI (interstimulus interval). Data reproduced, with permission, from Thomson (1997).

one has to consider their consequences for synaptic activity—the primary mode of transmission of information from one neuron to another. For example, is presentation of a number of spikes synchronously from multiple presynaptic neurons (a temporally coded pattern) as effective as an equal number of spikes from a single presynaptic source (a rate coded pattern)?

Two biophysical phenomena controlling synaptic efficacy are pertinent to this issue. First, the high degree of possible temporal precision seen during oscillations for neurons in vivo (Gray and Singer, 1989) and more reduced approaches (Mainen and Sejnowski, 1995) brings temporally coordinated inputs from multiple sources into the window in which supralinear summation of excitatory postsynaptic potentials (EPSPs) can occur. Multiple excitatory inputs onto principal cells can generate a postsynaptic response that is much greater than their algebraic sum (Nettleton and Spain, 2000; Fujisawa et al., 2008; Figure 4A). Spike timing precision between coactive peers needs to be ca. <5 ms—as seen in ascending inputs in both visual and auditory streams (Wang, 2010; Kayser et al., 2010). This timescale is partly related to active dendritic spiking (Losonczy and Magee, 2006) under control of potassium conductance (Nettleton and Spain, 2000; Goldberg et al., 2003).

Second, for single-neuron inputs, rate codes are at the mercy of short-term synaptic plasticity. Synaptic depression at excitatory neuron to excitatory neuron synapses predominates (e.g., Thomson, 1997; Thomson and Bannister, 1999; Thomson

et al., 2002; Williams and Atkinson, 2007; Figure 3B). The phenomenon is robust and involves both pre- and postsynaptic mechanisms such as sodium channel inactivation in intensely activated axons (e.g., Debanne, 2004), and release probability changes (Tsodyks and Markram, 1997). Depression of multiple postsynaptic responses from a single neuron is more evident for shorter interspike intervals, thus higher rates of spiking in a presynaptic neuron will have increasingly less of an effect on the postsynaptic neuron as the train progresses (Figure 4B). This phenomenon is not apparent for the first spike in a train though, perhaps in part explaining the observation that the first sensory-induced spike in a rate increase carries most information in vivo (Chase and Young, 2007; Panzeri et al., 2001). Synaptic depression is therefore a seemingly potent limitation on the time-window in which an increase in spike rate may carry information. However, transient, instantaneous increases in spike rates in a population (defined as the number of spikes in the population over a small time epoch) can reliably generate strong postsynaptic signals (Silberberg et al., 2004). On a larger scale, rapid transitions in EEG state have been proposed to flag cortical computation (Fingelkurts, 2010).

From the above, it appears that while increases in spike rate, in the absence of an overt temporal code, in many neurons in a population can readily generate assemblies (e.g., Figure 6B) the influence of assembly activity on target and peer neurons is time limited. Influence is maximal only in the first 5–10 ms of

rate increase. However, responses to sensory input outlast discrete stimuli by many 100s of ms (Altmann et al., 1986; Metherate and Cruikshank, 1999) to several seconds during short term memory tasks (Tallon Baudry et al., 1998). These longer responses are often accompanied by a clear signature of temporal coding, such as the gamma rhythm, whose basis in synaptic inhibition serves to time-limit postsynaptic effects of all but precisely timed concurrent inputs (e.g., Burchell et al., 1998). It is possible then to suggest that instantaneous changes in spike rates may dominate the cortical population code immediately on stimulus presentation, but that more persistent, iterative assembly formation via temporal, oscillation coding dominates thereafter. However, this does not per se rule out interaction between rate and temporal codes as sensory inputs often phase reset ongoing gamma rhythms. Thus, the initial spikes in a response to cortical input may already be part of a gamma-synchronized response (Fries et al., 2001).

### Gamma Rhythm Heterogeneity Provides Multiple Temporal Structures for Assembly Generation

While a pure rate code may be feasible as means to provide an initial cortical representation of sensory stimuli, one cannot rule out an interaction with gamma rhythms as a temporal code here either. Many different modes of gamma rhythm generation can be experimentally induced (Whittington et al., 2011), but none of the known manifestations truly behave as a “clock” for principal cell spike timing. Principal cell inputs to interneurons are vital to drive the observed rhythm and changes in principal cell spike behavior can alter the gamma rhythm on a period by period basis (Whittington et al., 1995). The main differences lie in the way fast spiking interneurons are recruited into the population rhythm by principal cells—they can be recruited by tonic excitation through glutamate overflow at synapses activating metabotropic receptors, convergence onto excitatory synapses on interneurons of ectopic action potentials generated in principal cell axons, or conventional somatic spike generation.

Persistent, highly frequency-inert gamma rhythms associate with sparse somatic spiking (Miller, 1996) in superficial neocortex. Gamma rhythms can also be generated in hippocampus that are associated with high spike rates in individual neurons (an order of magnitude greater than in persistent gamma rhythms) and are considerably more frequency—and thus spike rate—variable (Whittington et al., 1997). In neocortex, spike rates are closely related to gamma rhythm generation (in conjunction with slower changes in membrane potential (Mazzoni et al., 2010), with gamma rhythms being the single most important determinant of spike-density function (Rasch et al., 2008). But many *in vivo* studies show sensory-induced spike rate changes that peak at mean rates way above the classical gamma band frequency (e.g., Zinke et al., 2006). If it is assumed that spike timing is precisely determined by the trains of GABAergic inhibition that are the signature of population gamma rhythms, then how is this possible? One explanation for these data is that there are at least two gamma rhythm generators in neocortex.

First, a persistent rhythm provides relatively rigid temporal structure despite low principal cell spike rates and low population gamma frequencies (ca. 40 Hz). Such a rhythm has been documented in superficial layers of primary sensory and associ-

ation cortices (Cunningham et al., 2004; Ainsworth et al., 2011; Figure 5), where spike rates favor sparse coding (Wolfe et al., 2010). Such a scheme is particularly evident in local representations of sensory stimuli (Ohiorhenuan et al., 2010) where input increases quiescence but also increases temporally brief periods of common (population) activity. This sparseness has been proposed to be due to increases in surround inhibition (Haider et al., 2010), which is, in turn, related to the magnitude of observed gamma rhythm (Bartolo et al., 2011).

Second, a more frequency labile rhythm associated with large increases in principal cell spike rates on stimulation is seen (Uhlhaas et al., 2010). Using *in vitro* models of cortical activation, such a rhythm can be seen to coexist with the persistent rhythm described above, but with different laminar origins in primary sensory cortex (Figure 5). Low levels of excitation to primary auditory cortex generate a ca. 40 Hz gamma rhythm in layers 2/3. In this situation, layer 2/3 regular spiking (RS) neuron somatic outputs are sparse—in the order of a few Hz. In layer 4 somatic spiking is absent or also sparse, with membrane potential of stellate cells dominated by large-amplitude inhibitory postsynaptic potentials (IPSPs) at the superficial layer gamma frequency. However, if cortical excitation is increased an additional spectral peak, arising from layer 4, is seen in field potential data corresponding to the high gamma band (50–90 Hz; Figure 5). This granular layer gamma rhythm is associated with high principal cell spike rates and is locally variable in frequency of both the population field potential and individual neuronal action potential rates.

Similarly, frequency separated gamma generators are observed in entorhinal cortex and hippocampus (Colgin et al., 2009) and have been shown to correspond to different local circuits with differing laminar involvement of interneurons (Middleton et al., 2008). Both the neocortical rhythms described above are also inhibition based, being critically dependent on activation of GABA<sub>A</sub> receptor-mediated synaptic inhibition. However, the faster, more frequency-labile layer 4 gamma rhythm was significantly less dependent on phasic synaptic excitation and more on recurrent excitation via NR2C/D-containing NMDA receptors preferentially located on layer 4 principal cells (Binshtok et al., 2006; Ainsworth et al., 2011). Examining individual neuronal synaptic inputs and spike outputs also pointed to different local circuit processes. While principal cells in layers 2/3 spiked sparsely during the mixed gamma rhythm, they received robust synaptic inputs dominated by trains of IPSPs at the low gamma frequency (Ainsworth et al., 2011). The mismatch between somatic spike rates and intensity of phasic drive to interneurons is explained by ectopic action potential generation and propagation through gap-junction-coupled axons—a fundamental mechanism underlying persistent, low frequency gamma rhythms (Traub et al., 2000). Thus, the layer 2/3 low gamma rhythm resembled the persistent form of gamma driven by increased axonal action potential rates induced by kainate (Juuri et al., 2010), being gap junction and phasic excitation dependent. A separation of function for high and low gamma bands such as these has been preceded for a number of sensory modalities and cognitive tasks (Vidal et al., 2006; Wyart and Tallon Baudry, 2008; Kaiser et al., 2008; Herrmann et al., 2010).

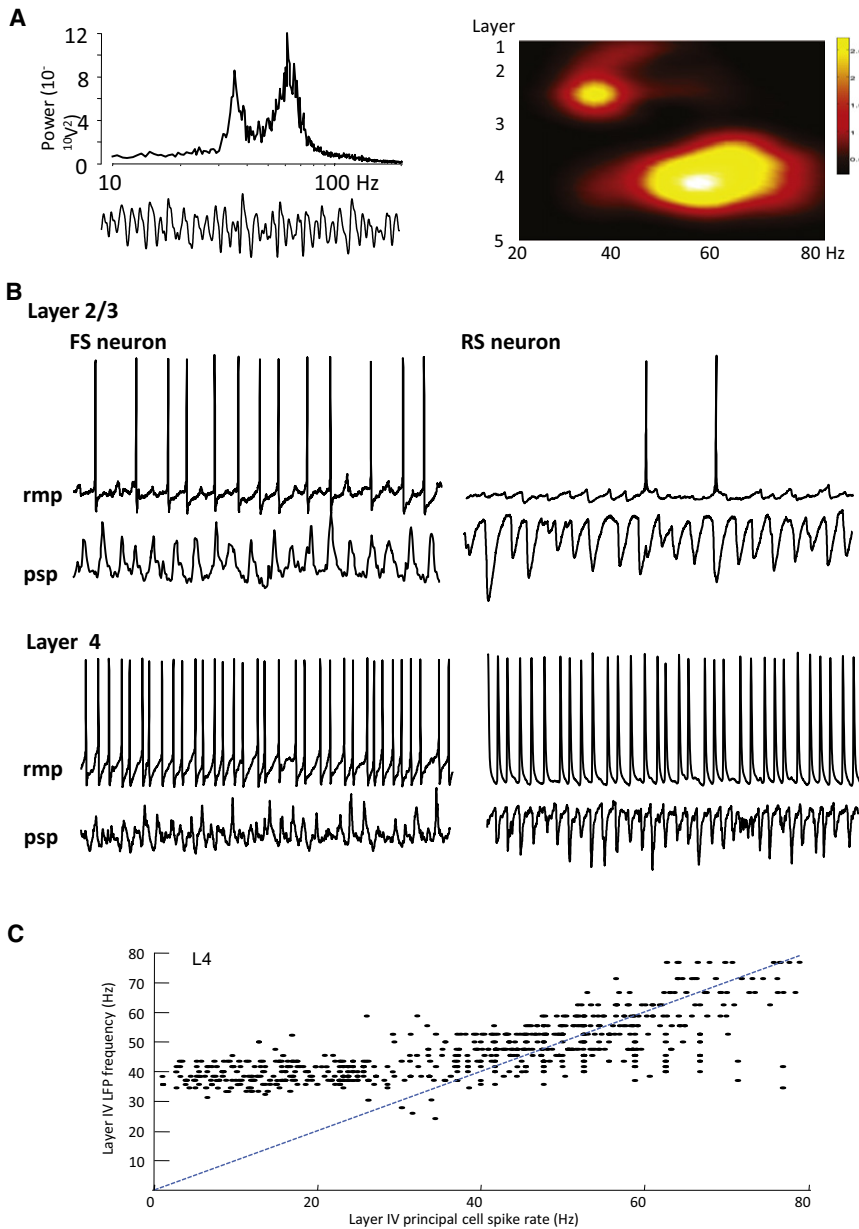


**Figure 5. Two Mechanistically and Frequency-Distinct Gamma Rhythms Coexist in Primary Auditory Cortex**

(A) Pooled power spectrum ( $n = 5$ ) of field potential activity recorded from upper layer 4 primary auditory cortex in the presence of  $0.8 \mu\text{M}$  kainate in vitro (Ainsworth et al., 2011). Below is a 0.5 s example of raw data. The two modal peak frequencies within the gamma band were distributed in a lamina-specific manner. Plotting mean power at peak frequency (colormap, dB above mean spectral power) against electrode laminar location and mean peak frequency shows both the layer 4 location of the high gamma rhythm and the broader frequency range compared with the layer 2/3 gamma rhythm.

(B) Example intracellular somatic recordings from layer 2/3 and layer 4 fast spiking interneurons (FS) and regular spiking principal cells (RS) during low or high gamma generation. Upper traces show 0.5 s examples of spiking in each cell type in layers 2/3 and the profile of EPSPs (FS neurons recorded from  $-70 \text{ mV}$ ) and IPSPs (RS neurons recorded from  $-30 \text{ mV}$ ) accompanying the field oscillation. Lower traces show corresponding recordings during layer 4. Note the faster frequency of RS neuron spike generation (almost one per period) and IPSP input. Note also the weaker, more irregular phasic excitatory synaptic input to layer 4 FS cells. Scale bar 20 mV (rmp), 5 mV (psp).

(C) Locally generated layer 4 gamma rhythms and gamma projected from layer 2/3 cause local field potential/spike dissociation depending on network frequency. Data show pairwise plots of data points for layer 4 cell interspike interval and concurrent instantaneous frequency of the local field potential (LFP). Note population frequency remains at ca. 40 Hz in layer 4 while layer 4 spike rates are relatively lower than this. Once spike rates increase the LFP frequency increases to match spike rate in the experimental conditions used (global activation of the region studied).

The presence of a fast, frequency-variable population gamma rhythm in the main target for ascending cortical input (layer 4) adds the intensity of spike generation associated with rate-coded phenomena to the highly precise temporal control of spike times seen with lower frequency gamma rhythms. The dominance of each type of temporal/rate code was seen to be dependent on the degree of excitation in layer 4, with the superficial layer population rhythm (temporal code) dictating activity in the layer 4 principal cell population until spike rates exceeded the layer 2/3 population rhythm frequency. Thereafter, further increases in excitation generated a population frequency in layer 4 that exceeded the layer 2/3 gamma frequency but closely matched individual principal cell spike rates closely (Figure 5C). The result is a means to iteratively (on a gamma

period-by-period basis) generate assemblies involving over 50% of coactive neurons (Figures 6C and 6E), without the broad distribution of spike times, relative between active units, in the population seen for increases in spike rate alone. It also provides a substrate for competitive interactions between coactivated neurons where more strongly excited layer 4 neurons (with higher spike rates) can suppress those receiving weaker input via lateral inhibition (Moran and Desimone, 1985; Börgers et al., 2005), a phenomenon not possible with sparse spiking at closely matched frequencies as seen in layers 2/3.

Different subtypes of gamma rhythm are seen in both auditory and visual cortex (Ainsworth et al., 2011; Oke et al., 2010). However, the precise laminar origin of the two components of the gamma band are different. This region-specific laminar distribution of different frequency subbands has also been reported for alpha rhythms (Bollimunta et al., 2008; Buffalo et al., 2011), suggesting region-specific, fundamentally different laminar organization of rhythmic activity. The presence of locally expressed, different population frequencies may in part provide

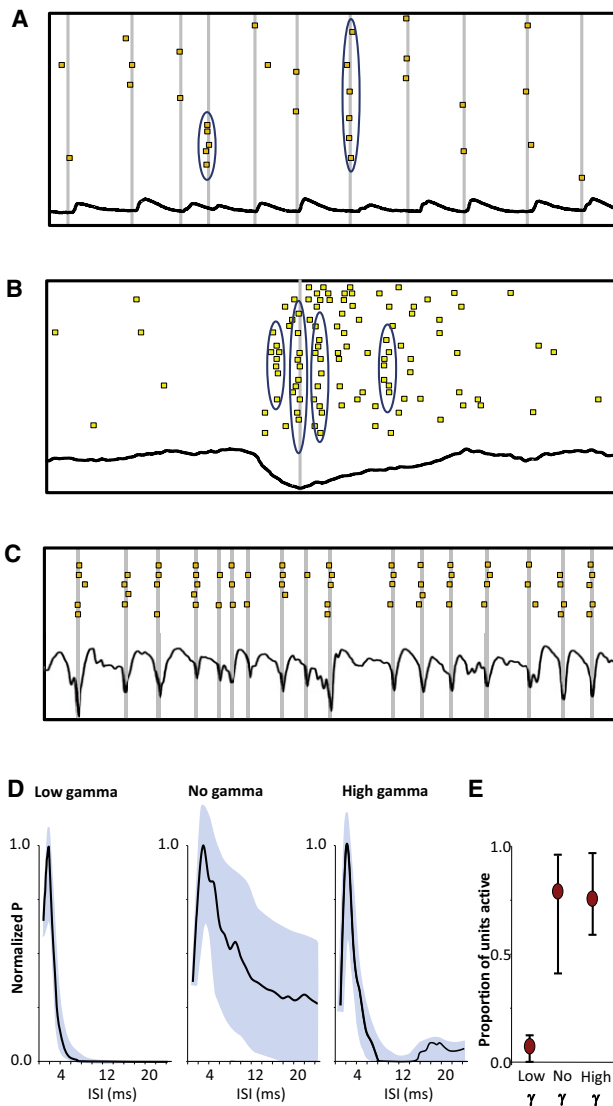


**Figure 6. Pyramidal Interneuron Network Gamma (PING) Combines High-Spike Rate Coding with Temporal Coding Associated with Gamma Rhythms**

(A) Example raster plot of spiking from 24 units recorded during persistent gamma rhythm generation in neocortex *in vitro*. Gamma was generated by 400 nM kainate and a 300 ms epoch of layer 2/3 field potential is superimposed for reference. Peak negativity of each field gamma period is shown by the gray lines. Note despite the very sparse spike incidence clear example of highly synchronous concurrent spike generation are evident (circled).

(B) Transient population bursts in neocortex generated by partial disinhibition. Graph shows raster plots for 23 concurrently recorded units along with a 300 ms field potential from layer 2/3. Peak field negativity of the transient is shown by the gray line. Note the intense (relative to A) but brief increase in spike rate for each unit, with nearly all units generating synchronous spikes around the field potential maximum deflection.

(C) Raster plot of spikes from 6 units in mid cortical layer and corresponding local field potential (300 ms epoch). Gray lines show the peak negativity in the field potential. Note most periods of the high gamma are accompanied by tightly synchronized spikes in most of the units recorded.

(D) Left panel, histogram of interspike interval (ISI) distribution *between* different units during persistent gamma rhythms in layer 2/3 neocortex *in vitro*. Data normalized to peak ISI incidence. SEM of the data is plotted as the blue band between upper and lower errors. Middle panel, histogram of interspike interval distribution *between* different units during transient population bursts

a possible substrate for some of the highly task-dependent, contrasting effects of spike timing and gamma rhythm power changes seen *in vivo* (Chalk et al., 2010; Fries et al., 2001) and higher frequency gamma “suppression” or enhancement during task performance depending on cortical subregion studied (Shmuel et al., 2006; Hayden et al., 2009; Jerbi et al., 2010).

### Consequences of Gamma Frequency Variance: Relation to Long-Term Plasticity

Gamma rhythms are reported to be involved in a number of correlates of memory (see Wang, 2010), as are neuronal assemblies (Dupret et al., 2010). Precise synchrony of spiking in anatomically disparate populations of neurons is ideal to take advantage of positive, short-term synaptic plastic phenomena favoring a temporal code (see above). However, the same cannot be said for long-term potentiation of synapses critical for linking Hebb’s original “fire together, wire together” proposals with useful substrates for storage and recall of information (e.g., Blumenfeld et al., 2006). Spike-timing-dependent plasticity (STDP) is near ubiquitous in cortex (Dan and Poo, 2006; Graupner and Brunel, 2010) and shows a marked discontinuity when pre- and postsynaptic spike time separations are zero. Thus, synchronous spiking in connected principal cells may result in postsynaptic activity preceding presynaptic activity (with a delay dependent on conduction time between each neuron) and *depressing* the synapses involved. Thus, systematic phase shifts between connected neurons or areas may potentially and bidirectionally alter the synaptic influence of one over the other (Vinck et al., 2010). Similarly, a rate code alone is unlikely to provide a robust means to selectively change synaptic weights in an STDP-dominated network given the lack of requirement for specific phase relationships between spikes in active neurons.

The synaptic depression likely in an STDP scheme with synchrony may, however, be computationally advantageous within assemblies and onto their targets. An enhancement of direction sensitivity, and perhaps other computations requiring both spatial and temporal neural components, is afforded by such gamma-induced synaptic depression in computational models (Carver et al., 2008). However, with dual gamma rhythm-generating circuits the situation becomes more complex. The combination of a highly frequency-stable superficial layer gamma generator with one of more considerable frequency variance in layer 4, dependent on excitatory input strength, suggests a range of frequency ratios. Such mismatched frequencies generate highly time-variable phase relationships between laminae that can differentially influence

(no gamma) in layer 2/3 neocortex *in vitro*. Note the much broader distribution of relative spike times between units and the greater variance in the data, particularly at longer ISI times illustrating the effect of oscillations in spike temporal precision (Schaefer et al., 2006). Right panel, mean ISI distribution histogram between different units during layer 4 high-frequency PING gamma generation.

(E) Median ( $\pm$ IQR) number of maximal units active within 5 ms of their peers for each of the network behaviors in (A)–(C). Note high gamma activity in layer 4 is associated with both the high temporal precision seen with low gamma rhythms and the high rate of closely temporally correlated spikes seen during transient bursts making it a very effective generator of neuronal assemblies. Figures adapted from Ainsworth et al. (2011).

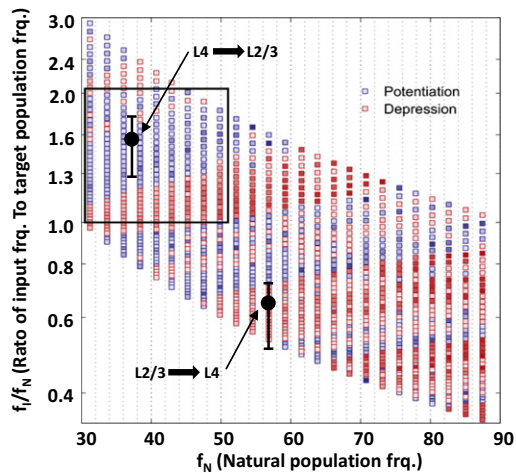


**Figure 7. Dual Local Gamma Rhythms Favor Intralaminar Synaptic Plasticity Mismatch**

Graph shows the pattern of spike-timing-dependent potentiation (blue squares) or depression (red squares) of NMDA receptor-containing synapses from principal cells in one gamma oscillating network to principal cells in an independent gamma oscillating network. The data are from conductance-based model simulations of pyramidal-interneuron network gamma rhythms and show clear bands of synaptic plasticity dependent upon both the ratio of the input ( $f_i$ ) and target network frequencies and the natural frequency ( $f_N$ ) of the target network. Overlaid are the mean  $\pm$ SEM frequency ratios for the layer 2/3 low gamma versus the layer 4 high gamma rhythms plotted at their natural frequencies (black circles). Note that the frequency mismatch between the two gamma rhythms favors potentiation of ascending inputs from layer 4 to layers 2/3 and not vice versa. Figure adapted and reproduced from Lee et al. (2009).

spike-timing-dependent plasticity. Interestingly, a computational model of just such a situation predicts marked changes in synaptic plasticity depending on precise frequency ratio (Lee et al., 2009). By focusing on a reduced model of assembly behavior including NMDA receptor-dependent STDP, the simulations predict that depression will occur with frequency-matching throughout the low gamma band (30–50 Hz; Figure 7). However, a higher frequency input, as seen for layer 4 to layer 2/3 projections during dual gamma rhythm generation) generates potentiation. The effect is highly direction selective, with the converse projection (layers 2/3 back to deeper layers) showing depression with such a frequency mismatch. Evidence for such connectivity (at least between excitatory neurons) is weak, but where seen it also shows a strong short term depression (Williams and Atkinson, 2007). These data together suggest a situation where dual gamma rhythm generation can selectively potentiate layer 4 to layer 2/3 connectivity only when neurons in layer 4 are strongly activated, but that the converse pathway is continually suppressed as long as the appropriate frequency differences are maintained.

### Summary

Is the concept of a spike timing-dependent population code likely to be useful in guiding future research hypotheses? The existence of multiple, frequency-labile gamma rhythm generators partly supports both sides of the arguments favoring rate versus temporal code. However, it also does not fit comfortably

with the idea of synchrony being predominant as a flag for active population coding. Considering phase space, the existence of two different frequencies of gamma rhythm goes beyond even the “synchrony versus sequence” concepts—the former providing a readily observable correlate of intercortical communication (Fries, 2005), the latter providing a robust means to address STDP issues (Aviel et al., 2005). Stable spike rate differences between coactive neuronal populations may result in time-variant phase relationships. These too can be manipulated to generate synaptic plastic effects (Lee et al., 2009), but their existence suggests the conventional definition of a neuronal assembly may merely be “tip of the iceberg” for the cortical computational code. Highly temporally precise spike times are easy to spot, as are rate changes. But at any time period during cortical activity a myriad of coexistent phase relationships and spike frequencies may manifest in a neuronal population (e.g., Canolty et al., 2010)—particularly when comparing concurrent activity patterns across different laminae. Unraveling the resultant spatiotemporal complexity may be vital to understand the true nature of cortical coding and computation but currently seem experimentally rather daunting. In this respect experimental approaches to understanding cortical function sample either too broadly (local field potentials) or with too much focus (a few spike trains). A move to more massively parallel neuronal recordings (e.g., the 4,096 electrode arrays used in vitro (Berdondini et al., 2005), with more focus on laminar interactions (e.g., Maier et al., 2010) may provide the data sets needed to take these thorny issues further.

### ACKNOWLEDGMENTS

The authors wish to thank The Wolfson Foundation and The EPSRC for support. M.A. is a doctoral student funded as part of the CARMEN e-science project. R.D.T. was supported by IBM, NIH/NINDS (NS44133, NS062955) and The Alexander von Humboldt Stiftung. N.J.K. and S.L. were supported by NSF DMS-0602204; N.J.K. was also supported by NSF-DMS-0717670 and NIH NINDS NS062955.

### REFERENCES

- Abeles, M. (1988). Neural codes for higher brain function. In *Information Processing by the Brain*, H.J. Markowitsch, ed. (Stuttgart: Hans Huber), pp. 225–238.
- Aggelopoulos, N.C., Franco, L., and Rolls, E.T. (2005). Object perception in natural scenes: encoding by inferior temporal cortex simultaneously recorded neurons. *J. Neurophysiol.* 93, 1342–1357.
- Ainsworth, M., Lee, S., Cunningham, M.O., Roopun, A.K., Traub, R.D., Kopell, N.J., and Whittington, M.A. (2011). Dual  $\gamma$  rhythm generators control interlaminar synchrony in auditory cortex. *J. Neurosci.* 31, 17040–17051.
- Altmann, L., Eckhorn, R., and Singer, W. (1986). Temporal integration in the visual system: influence of temporal dispersion on figure-ground discrimination. *Vision Res.* 26, 1949–1957.
- Andersen, R.A. (1995). Encoding of intention and spatial location in the posterior parietal cortex. *Cereb. Cortex* 5, 457–469.
- Anderson, J.C., Binzegger, T., Martin, K.A.C., and Rockland, K.S. (1998). The connection from cortical area V1 to V5: a light and electron microscopic study. *J. Neurosci.* 18, 10525–10540.
- Arenz, A., Silver, R.A., Schaefer, A.T., and Margrie, T.W. (2008). The contribution of single synapses to sensory representation in vivo. *Science* 321, 977–980.

- Arieli, A., Shoham, D., Hildesheim, R., and Grinvald, A. (1995). Coherent spatiotemporal patterns of ongoing activity revealed by real-time optical imaging coupled with single-unit recording in the cat visual cortex. *J. Neurophysiol.* *73*, 2072–2093.
- Aviel, Y., Horn, D., and Abeles, M. (2005). Memory capacity of balanced networks. *Neural Comput.* *17*, 691–713.
- Bartolo, M.J., Gieselmann, M.A., Vuksanovic, V., Hunter, D., Sun, L., Chen, X., Delicato, L.S., and Thiele, A. (2011). Stimulus-induced dissociation of neuronal firing rates and local field potential gamma power and its relationship to the resonance blood oxygen level-dependent signal in macaque primary visual cortex. *Eur. J. Neurosci.* <http://dx.doi.org/10.1111/j.1460-9568.2011.07877>.
- Beggs, J.M., and Plenz, D. (2003). Neuronal avalanches in neocortical circuits. *J. Neurosci.* *23*, 11167–11177.
- Berdondini, L., van der Wal, P.D., Guenat, O., de Rooij, N.F., Koudelka-Hep, M., Seitz, P., Kaufmann, R., Metzler, P., Blanc, N., and Rohr, S. (2005). High-density electrode array for imaging in vitro electrophysiological activity. *Biosens. Bioelectron.* *21*, 167–174.
- Biederlack, J., Castelo-Branco, M., Neuenschwander, S., Wheeler, D.W., Singer, W., and Nikić, D. (2006). Brightness induction: rate enhancement and neuronal synchronization as complementary codes. *Neuron* *52*, 1073–1083.
- Binshtok, A.M., Fleidervish, I.A., Sprengel, R., and Gutnick, M.J. (2006). NMDA receptors in layer 4 spiny stellate cells of the mouse barrel cortex contain the NR2C subunit. *J. Neurosci.* *26*, 708–715.
- Blumenfeld, B., Preminger, S., Sagi, D., and Tsodyks, M. (2006). Dynamics of memory representations in networks with novelty-facilitated synaptic plasticity. *Neuron* *52*, 383–394.
- Bollimunta, A., Chen, Y., Schroeder, C.E., and Ding, M. (2008). Neuronal mechanisms of cortical alpha oscillations in awake-behaving macaques. *J. Neurosci.* *28*, 9976–9988.
- Börgers, C., Epstein, S., and Kopell, N.J. (2005). Background gamma rhythmicity and attention in cortical local circuits: a computational study. *Proc. Natl. Acad. Sci. USA* *102*, 7002–7007.
- Börgers, C., Talei Franzesi, G., Lebeau, F.E., Boyden, E.S., and Kopell, N.J. (2012). Minimal size of cell assemblies coordinated by gamma oscillations. *PLoS Comput. Biol.* *8*, e1002362.
- Braitenberg, V. (1978). Cell assemblies in the cerebral cortex. In *Theoretical Approaches to Complex Systems*, R. Heim and G. Palm, eds. (New York: Springer), pp. 171–188.
- Brecht, M., Schneider, M., Sakmann, B., and Margrie, T.W. (2004). Whisker movements evoked by stimulation of single pyramidal cells in rat motor cortex. *Nature* *427*, 704–710.
- Budd, J.M.L. (1998). Extrastriate feedback to primary visual cortex in primates: a quantitative analysis of connectivity. *Proc. R. Soc. Lond. Ser. B* *265*, 1037–1044.
- Buffalo, E.A., Fries, P., Laandman, R., Buschman, T.J., and Desimone, R. (2011). Laminar differences in gamma and alpha coherence in the ventral stream. *Proc. Natl. Acad. Sci. USA* *108*, 11262–11267.
- Burchell, T.R., Faulkner, H.J., and Whittington, M.A. (1998). Gamma frequency oscillations gate temporally coded afferent inputs in the rat hippocampal slice. *Neurosci. Lett.* *255*, 151–154.
- Canolty, R.T., Ganguly, K., Kennerley, S.W., Cadieu, C.F., Koepsell, K., Wallis, J.D., and Carmena, J.M. (2010). Oscillatory phase coupling coordinates anatomically dispersed functional cell assemblies. *Proc. Natl. Acad. Sci. USA* *107*, 17356–17361.
- Carver, S., Roth, E., Cowan, N.J., and Fortune, E.S. (2008). Synaptic plasticity can produce and enhance direction selectivity. *PLoS Comput. Biol.* *4*, e32.
- Chalk, M., Herrero, J.L., Gieselmann, M.A., Delicato, L.S., Gotthardt, S., and Thiele, A. (2010). Attention reduces stimulus-driven gamma frequency oscillations and spike field coherence in V1. *Neuron* *66*, 114–125.
- Chase, S.M., and Young, E.D. (2007). First-spike latency information in single neurons increases when referenced to population onset. *Proc. Natl. Acad. Sci. USA* *104*, 5175–5180.
- Colgin, L.L., Denninger, T., Fyhn, M., Hafting, T., Bonnevie, T., Jensen, O., Moser, M.B., and Moser, E.I. (2009). Frequency of gamma oscillations routes flow of information in the hippocampus. *Nature* *462*, 353–357.
- Cunningham, M.O., Whittington, M.A., Bibbig, A., Roopun, A., LeBeau, F.E., Vogt, A., Monyer, H., Buhl, E.H., and Traub, R.D. (2004). A role for fast rhythmic bursting neurons in cortical gamma oscillations in vitro. *Proc. Natl. Acad. Sci. USA* *101*, 7152–7157.
- Dan, Y., and Poo, M.M. (2006). Spike timing-dependent plasticity: from synapse to perception. *Physiol. Rev.* *86*, 1033–1048.
- De Valois, R.L., Albrecht, D.G., and Thorell, L.G. (1982). Spatial frequency selectivity of cells in macaque visual cortex. *Vision Res.* *22*, 545–559.
- Debanne, D. (2004). Information processing in the axon. *Nat. Rev. Neurosci.* *5*, 304–316.
- deCharms, R.C., and Merzenich, M.M. (1996). Primary cortical representation of sounds by the coordination of action-potential timing. *Nature* *381*, 610–613.
- Deppisch, J., Pawelzik, K., and Geisel, T. (1994). Uncovering the synchronization dynamics from correlated neuronal activity quantifies assembly formation. *Biol. Cybern.* *71*, 387–399.
- Deuchars, J., and Thomson, A.M. (1996). CA1 pyramid-pyramid connections in rat hippocampus in vitro: dual intracellular recordings with biocytin filling. *Neuroscience* *74*, 1009–1018.
- Dupret, D., O’Neill, J., Pleydell-Bouverie, B., and Csicsvari, J. (2010). The reorganization and reactivation of hippocampal maps predict spatial memory performance. *Nat. Neurosci.* *13*, 995–1002.
- Duret, F., Shumikhina, S., and Molotchnikoff, S. (2006). Neuron participation in a synchrony-encoding assembly. *BMC Neurosci.* *7*, 72.
- Eckhorn, R., Bauer, R., Jordan, W., Brosch, M., Kruse, W., Munk, M., and Reitboeck, H.J. (1988). Coherent oscillations: a mechanism of feature linking in the visual cortex? Multiple electrode and correlation analyses in the cat. *Biol. Cybern.* *60*, 121–130.
- Eichenbaum, H. (1993). Thinking about brain cell assemblies. *Science* *261*, 993–994.
- Engel, A.K., Fries, P., and Singer, W. (2001). Dynamic predictions: oscillations and synchrony in top-down processing. *Nat. Rev. Neurosci.* *2*, 704–716.
- Fingelkurts, A.A. (2010). Topographic mapping of rapid transitions in EEG multiple frequencies: EEG frequency domain of operational synchrony. *Neurosci. Res.* *68*, 207–224.
- Freiwald, W.A., Kreiter, A.K., and Singer, W. (2001). Synchronization and assembly formation in the visual cortex. *Prog. Brain Res.* *130*, 111–140.
- Fries, P. (2005). A mechanism for cognitive dynamics: neuronal communication through neuronal coherence. *Trends Cogn. Sci.* *9*, 474–480.
- Fries, P., Roelfsema, P.R., Engel, A.K., König, P., and Singer, W. (1997). Synchronization of oscillatory responses in visual cortex correlates with perception in interocular rivalry. *Proc. Natl. Acad. Sci. USA* *94*, 12699–12704.
- Fries, P., Reynolds, J.H., Rorie, A.E., and Desimone, R. (2001). Modulation of oscillatory neuronal synchronization by selective visual attention. *Science* *291*, 1560–1563.
- Fritz, J., Shamma, S., Elhilali, M., and Klein, D. (2003). Rapid task-related plasticity of spectrotemporal receptive fields in primary auditory cortex. *Nat. Neurosci.* *6*, 1216–1223.
- Fujisawa, S., Amarasingham, A., Harrison, M.T., and Buzsáki, G. (2008). Behavior-dependent short-term assembly dynamics in the medial prefrontal cortex. *Nat. Neurosci.* *11*, 823–833.
- Goldberg, J.H., Tamas, G., and Yuste, R. (2003). Ca<sup>2+</sup> imaging of mouse neocortical interneurone dendrites: Ia-type K<sup>+</sup> channels control action potential backpropagation. *J. Physiol.* *551*, 49–65.

- Graupner, M., and Brunel, N. (2010). Mechanisms of induction and maintenance of spike-timing dependent plasticity in biophysical synapse models. *Front. Comput. Neurosci.* 17, 4.
- Gray, C.M., and Singer, W. (1989). Stimulus-specific neuronal oscillations in orientation columns of cat visual cortex. *Proc. Natl. Acad. Sci. USA* 86, 1698–1702.
- Haider, B., Krause, M.R., Duque, A., Yu, Y., Touryan, J., Mazer, J.A., and McCormick, D.A. (2010). Synaptic and network mechanisms of sparse and reliable visual cortical activity during nonclassical receptive field stimulation. *Neuron* 65, 107–121.
- Harris, K.D., Csicsvari, J., Hirase, H., Dragoi, G., and Buzsáki, G. (2003). Organization of cell assemblies in the hippocampus. *Nature* 424, 552–556.
- Hayden, B.Y., Smith, D.V., and Platt, M.L. (2009). Electrophysiological correlates of default-mode processing in macaque posterior cingulate cortex. *Proc. Natl. Acad. Sci. USA* 106, 5948–5953.
- Hebb, D.O. (1949). *The Organisation of Behaviour: A Neuropsychological Theory* (New York: Wiley).
- Herrmann, C.S., Fründ, I., and Lenz, D. (2010). Human gamma-band activity: a review on cognitive and behavioral correlates and network models. *Neurosci. Biobehav. Rev.* 34, 981–992.
- Holmgren, C., Harkany, T., Svennenfors, B., and Zilberter, Y. (2003). Pyramidal cell communication within local networks in layer 2/3 of rat neocortex. *J. Physiol.* 551, 139–153.
- Hormuzdi, S.G., Pais, I., LeBeau, F.E., Towers, S.K., Rozov, A., Buhl, E.H., Whittington, M.A., and Monyer, H. (2001). Impaired electrical signaling disrupts gamma frequency oscillations in connexin 36-deficient mice. *Neuron* 31, 487–495.
- Hubel, D.H., and Wiesel, T.N. (1959). Receptive fields of single neurones in the cat's striate cortex. *J. Physiol.* 148, 574–591.
- Huber, D., Petreanu, L., Ghitani, N., Ranade, S., Hromádka, T., Mainen, Z., and Svoboda, K. (2008). Sparse optical microstimulation in barrel cortex drives learned behaviour in freely moving mice. *Nature* 451, 61–64.
- Jerbi, K., Vidal, J.R., Ossandon, T., Dalal, S.S., Jung, J., Hoffmann, D., Minotti, L., Bertrand, O., Kahane, P., and Lachaux, J.P. (2010). Exploring the electrophysiological correlates of the default-mode network with intracerebral EEG. *Front. Syst. Neurosci.* 4, 27.
- Juuri, J., Clarke, V.R., Lauri, S.E., and Taira, T. (2010). Kainate receptor-induced ectopic spiking of CA3 pyramidal neurons initiates network bursts in neonatal hippocampus. *J. Neurophysiol.* 104, 1696–1706.
- Kaiser, J., Heidegger, T., Wibrall, M., Altmann, C.F., and Lutzenberger, W. (2008). Distinct gamma-band components reflect the short-term memory maintenance of different sound lateralization angles. *Cereb. Cortex* 18, 2286–2295.
- Kayser, C., Logothetis, N.K., and Panzeri, S. (2010). Millisecond encoding precision of auditory cortex neurons. *Proc. Natl. Acad. Sci. USA* 107, 16976–16981.
- Lamme, V.A., and Spekreijse, H. (1998). Neuronal synchrony does not represent texture segregation. *Nature* 396, 362–366.
- Lee, S., Sen, K., and Kopell, N. (2009). Cortical gamma rhythms modulate NMDAR-mediated spike timing dependent plasticity in a biophysical model. *PLoS Comput. Biol.* 5, e1000602.
- Levy, R.B., Reyes, A.D., and Aoki, C. (2006). Nicotinic and muscarinic reduction of unitary excitatory postsynaptic potentials in sensory cortex; dual intracellular recording in vitro. *J. Neurophysiol.* 95, 2155–2166.
- Logothetis, N.K., Pauls, J., and Poggio, T. (1995). Shape representation in the inferior temporal cortex of monkeys. *Curr. Biol.* 5, 552–563.
- Losonczy, A., and Magee, J.C. (2006). Integrative properties of radial oblique dendrites in hippocampal CA1 pyramidal neurons. *Neuron* 50, 291–307.
- Maier, A., Adams, G.K., Aura, C., and Leopold, D.A. (2010). Distinct superficial and deep laminar domains of activity in the visual cortex during rest and stimulation. *Front. Syst. Neurosci.* 4, 31.
- Mainen, Z.F., and Sejnowski, T.J. (1995). Reliability of spike timing in neocortical neurons. *Science* 268, 1503–1506.
- Markowitz, D.A., Collman, F., Brody, C.D., Hopfield, J.J., and Tank, D.W. (2008). Rate-specific synchrony: using noisy oscillations to detect equally active neurons. *Proc. Natl. Acad. Sci. USA* 105, 8422–8427.
- Mazzoni, A., Whittingstall, K., Brunel, N., Logothetis, N.K., and Panzeri, S. (2010). Understanding the relationships between spike rate and delta/gamma frequency bands of LFPs and EEGs using a local cortical network model. *Neuroimage* 52, 956–972.
- McAllister, L.B., Scheller, R.H., Kandel, E.R., and Axel, R. (1983). In situ hybridization to study the origin and fate of identified neurons. *Science* 222, 800–808.
- Metherate, R., and Cruikshank, S.J. (1999). Thalamocortical inputs trigger a propagating envelope of gamma-band activity in auditory cortex in vitro. *Exp. Brain Res.* 126, 160–174.
- Middleton, S., Jalics, J., Kispersky, T., Lebeau, F.E., Roopun, A.K., Kopell, N.J., Whittington, M.A., and Cunningham, M.O. (2008). NMDA receptor-dependent switching between different gamma rhythm-generating microcircuits in entorhinal cortex. *Proc. Natl. Acad. Sci. USA* 105, 18572–18577.
- Miller, R. (1996). Neural assemblies and laminar interactions in the cerebral cortex. *Biol. Cybern.* 75, 253–261.
- Moran, J., and Desimone, R. (1985). Selective attention gates visual processing in the extrastriate cortex. *Science* 229, 782–784.
- Nettleton, J.S., and Spain, W.J. (2000). Linear to supralinear summation of AMPA-mediated EPSPs in neocortical pyramidal neurons. *J. Neurophysiol.* 83, 3310–3322.
- Ochierhuan, I.E., Mechler, F., Purpura, K.P., Schmid, A.M., Hu, Q., and Victor, J.D. (2010). Sparse coding and high-order correlations in fine-scale cortical networks. *Nature* 466, 617–621.
- Oke, O.O., Magony, A., Anver, H., Ward, P.D., Jiruska, P., Jefferys, J.G., and Vreugdenhil, M. (2010). High-frequency gamma oscillations coexist with low-frequency gamma oscillations in the rat visual cortex in vitro. *Eur. J. Neurosci.* 31, 1435–1445.
- Olufsen, M.S., Whittington, M.A., Camperi, M., and Kopell, N.J. (2003). New roles for the gamma rhythm: population tuning and preprocessing for the Beta rhythm. *J. Comput. Neurosci.* 14, 33–54.
- Palm, G. (1990). Cell assemblies as a guideline for brain research. *Concepts Neurosci.* 1, 133–147.
- Panzeri, S., Petersen, R.S., Schultz, S.R., Lebedev, M., and Diamond, M.E. (2001). The role of spike timing in the coding of stimulus location in rat somatosensory cortex. *Neuron* 29, 769–777.
- Peters, A., and Payne, B.R. (1993). Numerical relationships between geniculocortical afferents and pyramidal cell modules in cat primary visual cortex. *Cereb. Cortex* 3, 69–78.
- Plenz, D., and Thiagarajan, T.C. (2007). The organizing principles of neuronal avalanches: cell assemblies in the cortex? *Trends Neurosci.* 30, 101–110.
- Pouille, F., and Scanziani, M. (2001). Enforcement of temporal fidelity in pyramidal cells by somatic feed-forward inhibition. *Science* 293, 1159–1163.
- Quiroga, R.Q., Reddy, L., Kreiman, G., Koch, C., and Fried, I. (2005). Invariant visual representation by single neurons in the human brain. *Nature* 435, 1102–1107.
- Rasch, M.J., Gretton, A., Murayama, Y., Maass, W., and Logothetis, N.K. (2008). Inferring spike trains from local field potentials. *J. Neurophysiol.* 99, 1461–1476.
- Riehle, A., Grammont, F., Diesmann, M., and Grün, S. (2000). Dynamical changes and temporal precision of synchronized spiking activity in monkey motor cortex during movement preparation. *J. Physiol. Paris* 94, 569–582.
- Roelfsema, P.R., Lamme, V.A., and Spekreijse, H. (2004). Synchrony and covariation of firing rates in the primary visual cortex during contour grouping. *Nat. Neurosci.* 7, 982–991.
- Roopun, A.K., Kramer, M.A., Carracedo, L.M., Kaiser, M., Davies, C.H., Traub, R.D., Kopell, N.J., and Whittington, M.A. (2008). Period concatenation

- underlies interactions between gamma and beta rhythms in neocortex. *Front. Cell. Neurosci.* 2, 1.
- Sakurai, Y. (1998). The search for cell assemblies in the working brain. *Behav. Brain Res.* 91, 1–13.
- Scannell, J.W., and Young, M.P. (1999). Primary visual cortex within the cortico-cortico-thalamic network. In *Cerebral Cortex*, Vol. 15. Cat Primary Visual Cortex, A. Peters, E.G. Jones, and B.R. Payne, eds. (New York: Plenum).
- Schaefer, A.T., Angelo, K., Spors, H., and Margrie, T.W. (2006). Neuronal oscillations enhance stimulus discrimination by ensuring action potential precision. *PLoS Biol.* 4, e163.
- Shadlen, M.N., and Movshon, J.A. (1999). Synchrony unbound: a critical evaluation of the temporal binding hypothesis. *Neuron* 24, 67–77, 111–125.
- Shadlen, M.N., and Newsome, W.T. (1994). Noise, neural codes and cortical organization. *Curr. Opin. Neurobiol.* 4, 569–579.
- Shadlen, M.N., and Newsome, W.T. (1995). Is there a signal in the noise? *Curr. Opin. Neurobiol.* 5, 248–250.
- Shmuel, A., Augath, M., Oeltermann, A., and Logothetis, N.K. (2006). Negative functional MRI response correlates with decreases in neuronal activity in monkey visual area V1. *Nat. Neurosci.* 9, 569–577.
- Silberberg, G., Wu, C., and Markram, H. (2004). Synaptic dynamics control the timing of neuronal excitation in the activated neocortical microcircuit. *J. Physiol.* 556, 19–27.
- Singer, W. (2010). Neocortical rhythms: an overview. In *Dynamic Coordination in the Brain*, C. von der Malsburg, W.A. Phillips, and W. Singer, eds. (Cambridge, MA: MIT Press), pp. 159–168.
- Singer, W., and Gray, C.M. (1995). Visual feature integration and the temporal correlation hypothesis. *Annu. Rev. Neurosci.* 18, 555–586.
- Smith, S.L., and Häusser, M. (2010). Parallel processing of visual space by neighboring neurons in mouse visual cortex. *Nat. Neurosci.* 13, 1144–1149.
- Smith, M.L., Gosselin, F., and Schyns, P.G. (2006). Perceptual moments of conscious visual experience inferred from oscillatory brain activity. *Proc. Natl. Acad. Sci. USA* 103, 5626–5631.
- Softky, W.R. (1995). Simple codes versus efficient codes. *Curr. Opin. Neurobiol.* 5, 239–247.
- Softky, W.R., and Koch, C. (1993). The highly irregular firing of cortical cells is inconsistent with temporal integration of random EPSPs. *J. Neurosci.* 13, 334–350.
- Tallon-Baudry, C., Bertrand, O., Peronnet, F., and Pernier, J. (1998). Induced gamma-band activity during the delay of a visual short-term memory task in humans. *J. Neurosci.* 18, 4244–4254.
- Thomson, A.M. (1997). Activity-dependent properties of synaptic transmission at two classes of connections made by rat neocortical pyramidal axons in vitro. *J. Physiol.* 502, 131–147.
- Thomson, A.M., and Bannister, A.P. (1999). Release-independent depression at pyramidal inputs onto specific cell targets: dual recordings in slices of rat cortex. *J. Physiol.* 519, 57–70.
- Thomson, A.M., West, D.C., Wang, Y., and Bannister, A.P. (2002). Synaptic connections and small circuits involving excitatory and inhibitory neurons in layers 2–5 of adult rat and cat neocortex: triple intracellular recordings and biocytin labelling in vitro. *Cereb. Cortex* 12, 936–953.
- Traub, R.D., Bibbig, A., Fisahn, A., LeBeau, F.E., Whittington, M.A., and Buhl, E.H. (2000). A model of gamma-frequency network oscillations induced in the rat CA3 region by carbachol in vitro. *Eur. J. Neurosci.* 12, 4093–4106.
- Traub, R.D., Cunningham, M.O., Gloveli, T., LeBeau, F.E., Bibbig, A., Buhl, E.H., and Whittington, M.A. (2003). GABA-enhanced collective behavior in neuronal axons underlies persistent gamma-frequency oscillations. *Proc. Natl. Acad. Sci. USA* 100, 11047–11052.
- Tsodyks, M.V., and Markram, H. (1997). The neural code between neocortical pyramidal neurons depends on neurotransmitter release probability. *Proc. Natl. Acad. Sci. USA* 94, 719–723.
- Uhlhaas, P.J., Pipa, G., Neuenschwander, S., Wibral, M., and Singer, W. (2010). A new look at gamma? High- (>60 Hz)  $\gamma$ -band activity in cortical networks: function, mechanisms and impairment. *Prog. Biophys. Mol. Biol.* 105, 14–28.
- Vaadia, E., Haalman, I., Abeles, M., Bergman, H., Prut, Y., Slovin, H., and Aertsen, A. (1995). Dynamics of neuronal interactions in monkey cortex in relation to behavioural events. *Nature* 373, 515–518.
- Vidal, J.R., Chaumon, M., O'Regan, J.K., and Tallon-Baudry, C. (2006). Visual grouping and the focusing of attention induce gamma-band oscillations at different frequencies in human magnetoencephalogram signals. *J. Cogn. Neurosci.* 18, 1850–1862.
- Vinck, M., Lima, B., Womelsdorf, T., Oostenveld, R., Singer, W., Neuenschwander, S., and Fries, P. (2010). Gamma-phase shifting in awake monkey visual cortex. *J. Neurosci.* 30, 1250–1257.
- Wang, X.J. (2010). Neurophysiological and computational principles of cortical rhythms in cognition. *Physiol. Rev.* 90, 1195–1268.
- Whittington, M.A., Traub, R.D., and Jefferys, J.G. (1995). Synchronized oscillations in interneuron networks driven by metabotropic glutamate receptor activation. *Nature* 373, 612–615.
- Whittington, M.A., Stanford, I.M., Colling, S.B., Jefferys, J.G., and Traub, R.D. (1997). Spatiotemporal patterns of gamma frequency oscillations tetanically induced in the rat hippocampal slice. *J. Physiol.* 502, 591–607.
- Whittington, M.A., Cunningham, M.O., LeBeau, F.E., Racca, C., and Traub, R.D. (2011). Multiple origins of the cortical  $\gamma$  rhythm. *Dev. Neurobiol.* 71, 92–106.
- Williams, S.R., and Atkinson, S.E. (2007). Pathway-specific use-dependent dynamics of excitatory synaptic transmission in rat intracortical circuits. *J. Physiol.* 585, 759–777.
- Wolfe, J., Houweling, A.R., and Brecht, M. (2010). Sparse and powerful cortical spikes. *Curr. Opin. Neurobiol.* 20, 306–312.
- Womelsdorf, T., Fries, P., Mitra, P.P., and Desimone, R. (2006). Gamma-band synchronization in visual cortex predicts speed of change detection. *Nature* 439, 733–736.
- Wyart, V., and Tallon-Baudry, C. (2008). Neural dissociation between visual awareness and spatial attention. *J. Neurosci.* 28, 2667–2679.
- Young, M.P. (2000). The architecture of visual cortex and inferential processes in vision. *Spat. Vis.* 13, 137–146.
- Zinke, W., Roberts, M.J., Guo, K., McDonald, J.S., Robertson, R., and Thiele, A. (2006). Cholinergic modulation of response properties and orientation tuning of neurons in primary visual cortex of anaesthetized Marmoset monkeys. *Eur. J. Neurosci.* 24, 314–328.